A Planar Hall Thruster for Investigating Electron Mobility in ExB Devices

IEPC-2007-187

Presented at the 30th International Electric Propulsion Conference, Florence, Italy
September 17-20, 2007

Joshua L. Rovey,* Matthew P. Giacomi,† Robert A. Stubbers,‡ and Brian E. Jurczyk§
Starfire Industries LLC, Champaign, IL. 61820

Abstract: Stable operation of a Hall thruster that emits and collects the Hall current across a planar discharge channel is described. The planar Hall thruster (PHT) is being investigated for use as a test bed to study electron mobility in ExB devices. The planar geometry attempts to de-couple the complex electron motion found in annular thrusters by using simplified geometry. During this initial test, the PHT was operated at discharge voltages between 50-150 V to verify operability and stability of the device. Hall current was emitted by hollow cathode electron sources and collected by electrodes on the opposing wall of the thruster. Internal channel wall probes along with a downstream Faraday probe and retarding potential analyzer measured changes in thruster plasma as the Hall current, discharge voltage, magnetic field, and mass flow rates were changed. Results show that most of the plume ions are created in the acceleration zone. Further, increasing the magnetic field confines electrons to the Hall-drift region. This causes the Hall current to increase and the discharge current to decrease. Future experiments with this thruster are being planned to shed light on electron mobility in both planar and annular ExB geometry.

Nomenclature

B	=	magnetic field strength
B_{max}	=	maximum magnetic field strength along the thruster centerlines
I_d	=	discharge current
$Mdot_A$	=	anode mass flow rate
$Mdot_E$	=	total emitter mass flow rate
TP	=	thruster point
V_d	=	discharge voltage
V_{wcp1}	=	collector wall probe floating voltage
V_{wcp2}	=	collector wall probe floating voltage
V_{wep3}	=	emitter wall probe floating voltage
V_{wep4}	=	emitter wall probe floating voltage

I. Introduction

HALL-EFFECT thrusters (HETs) are a type of space propulsion device that use electric fields to accelerate and expel ionized propellant to generate thrust. A schematic of an HET is shown in Figure 1 A HET is a coaxial device that utilizes a radial magnetic field crossed with an axial electric field. Electrons emitted by the cathode drift

* Propulsion Research Engineer, 60 Hazelwood Drive, Suite 143/203A, AIAA Member.
† Research Engineer, 60 Hazelwood Drive, Suite 143/203A.
‡ Vice President, 60 Hazelwood Drive, Suite 143/203A, AIAA Member.
§ President, 60 Hazelwood Drive, Suite 143/203A, AIAA Member.

in the $\vec{E} \times \vec{B}$ direction, forming an azimuthal Hall current. Neutral xenon atoms injected through the anode collide with these electrons producing xenon ions that are subsequently accelerated by the electric field to produce thrust. The magnitude of the magnetic field is designed such that only the electrons are magnetized. A mixture of electrons and ions in the acceleration zone creates a quasi-neutral plasma and thus the operation of the HET is not space-charge limited in ion current density as is the case with gridded ion thrusters.

Transverse electron mobility represents a loss in efficiency of the device, so ideally electrons would be confined to drift in the Hall current indefinitely. Unfortunately this is not realizable in practice and electrons do migrate to the anode. Furthermore, axial mobility cannot be characterized by a purely classical collisional diffusion model. In fact, experimental measurements in the SPT-100 have shown that the electron collision frequency is on the order of 107-108 Hz.1 Calculations from both internal and global measurements have shown that the collision frequency based off classical theory is 1,000 times lower.2 Because of this discrepancy, the term "anomalous" mobility has been used to describe the increased axial mobility present in cross-field devices such as HETs.3 Explanations of the "anomalous" mobility have been suggested and two main candidates are plasma turbulence2,4 and wall-effects.5-7 More efficient HETs that better confine Hall current electrons may be possible if a clearer understanding of the mobility in these devices is developed. With this in mind, Starfire Industries, LLC is using both numerical modeling and experiment to investigate and study electron mobility in HETs.

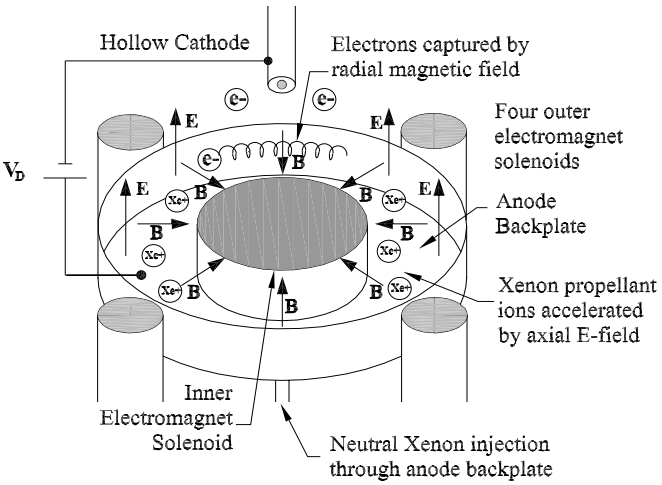

Figure 1. Schematic of a traditional, annular Hall-effect thruster.

A planar Hall thruster (PHT) is being investigated for use as a test bed to study electron mobility in ExB devices. The planar geometry attempts to de-couple the complex electron motion found in annular thrusters by using a simplified geometry. Annular HETs are known to contain complex electron motions resulting from gradients in the magnetic field, curvature drifts, radial electric fields, and magnetic mirror phenomena. These effects can lead to electron drifts, plasma instability, and wall cascades that limit device performance. The goal of the PHT is to remove some of the complexity resulting from the annular geometry to better study electron motion in ExB fields. The rectilinear design effectively eliminates the curvature-induced electron transport losses present in the annular system; however, there is the challenge of dealing with the accumulated Hall current since the system is not "closed drift". To solve this problem, the electron Hall current is injected into the acceleration region of the thruster through a port in the sidewall of the thruster channel ceramic. On the opposite side of the channel, a series of segmented electrodes capture the injected Hall current and recirculate this charge for re-injection on the opposite side.

The initial experiment presented here was designed to assess the operational stability and functionality of the PHT. Specific questions to be addressed were 1) will the PHT geometry and setup produce a stable plasma discharge; 2) can the Hall current be emitted and collected across the channel; and 3) what is the shape of the thruster beam profile? The following sections describe the PHT experimental apparatus, results, and conclusions regarding this investigation.

II. Experimental Apparatus and Setup

The PHT was operated in a high-vacuum facility over a week long test. The following sections describe the thruster, facility, and diagnostics used to complete the tests.

A. Hall Thruster

The PHT does not have the annular shape of the conventional Hall thruster. Rather, the device is planar (or linear) and Hall current is emitted at a sidewall and collected at the other end after traveling across the channel. Due to its geometry, there is no definitive "axis." However, the axial direction referenced below is the direction normal to the anode in the middle of the thruster. The front poles are thick and do not provide a sharp B_{max} as in conventional Hall thrusters. The magnetic circuit was designed this way to allow simple mounting of off-the-shelf

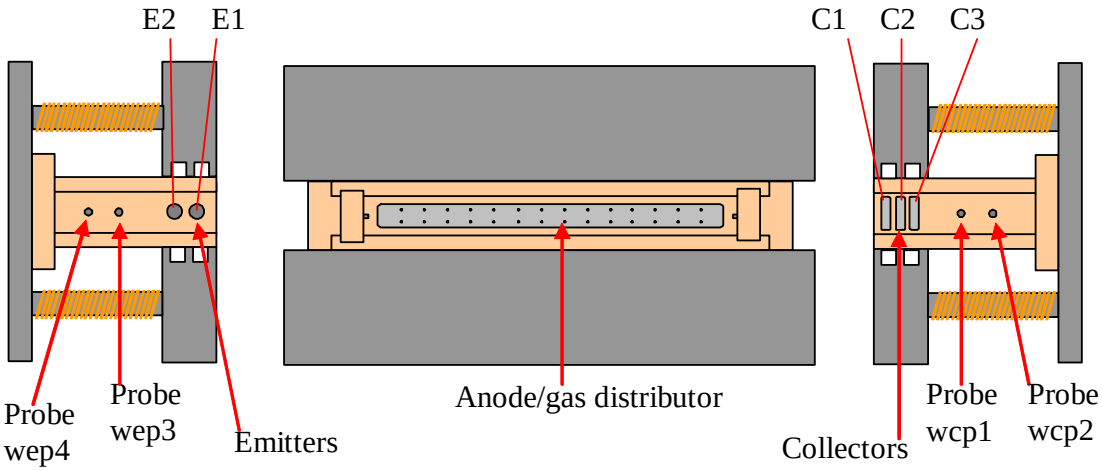

Figure 2. Schematics of the PHT . The left picture shows the emitter side of the channel. The center picture looks into the channel. The right picture looks at the collector side of the thruster.

electron sources in the Hall-drift (high B-field) region of the channel. A schematic is shown in Figure 2. The electromagnet circuit is made of low carbon steel and copper wire. The channel material is fired alumina silicate. The channel was constructed by sliding five plates together into recessed joints. The anode is stainless steel and also serves as a gas-distributor. A photograph of the thruster before and during operation is shown in Figure 3.

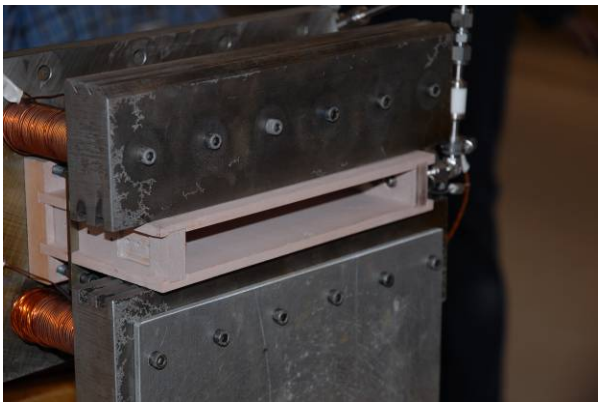

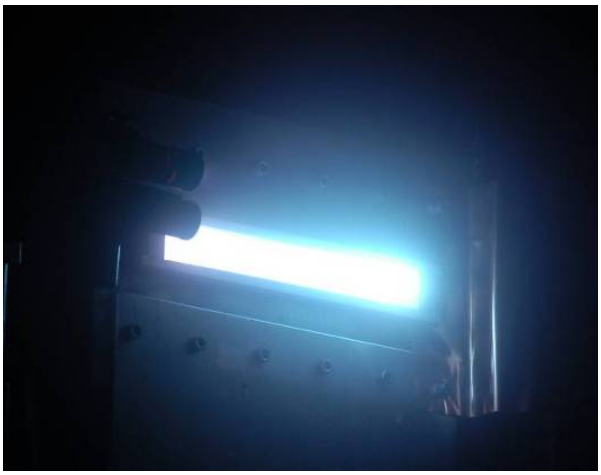

Figure 3. PHT before (top) and during (bottom) operation in the vacuum test facility.

1. Discharge Channel

The channel is constructed of baked alumina silicate ceramic plates. Its length, width, and depth are 203 mm, 25 mm and 108 mm, respectively. All electrodes are recessed into the ceramic plates. All joints are recessed as well, to minimize propellant leakage. In addition to the emitters and collectors, there are four Langmuir probes, two in each side wall. The walls are held in place by tongues on the emitter and collector sides, bolted to the main pole piece.

2. Magnetic Circuit

The magnetic circuit is made of low-carbon steel with a relative permeability of approximately 3000. The back pole piece is a 12-mm-thick, 203 mm by 305 mm plate. Twelve 83-mm-long, 19-mm-diameter posts are welded to the main pole and wound in series with approximately 100 m of copper wire. The front poles are bolted to the posts. The top and bottom front pole pieces are each 76-mm-wide, 38-mm-thick, and 305-mm-long. Two grooves are cut into each pole along their length, facing the channel to improve mirror confinement of electrons. Between the two front poles, the magnetic field is roughly 60 G per ampere of magnet wire current. The poles extend further than the channel so that edge effects are minimized. The back pole

piece also contains a hole bored for the anode/gas feed connection as well as eight holes for mounting. There is no magnetic shield and there are no trim coils. The electromagnet current conductor is 18 AWG Kapton coated copper wire. The wire begins to warm when currents reach 8 A (outside of vacuum). At this current, the magnetic field strength in the center of the channel is 500 Gauss.

3. Anode

The anode is a stainless steel gas manifold. The gas distributor has one inlet (centered) and approximately 30 holes without ballast. It nearly fills the channel cross-section. Each of the holes was bored through a 3.2-mm-thick bar of stainless steel. That bar was then welded onto the gas inlet/reservoir.

4. Channel Wall Emitter Cathodes

The emitters are hollow dispenser cathodes. They are 6.4-mm-diameter tantalum tubes with a stainless steel gas connection and a shielded heater. They are inserted through the wall and protrude into the channel 1-3 mm. Xenon was used as the working gas. The heater drives a tantalum emitter to thermionically emit electrons inside the cathode. The electrons are dispensed through a small orifice approximately 3.2 mm in diameter. Electron extraction is provided by titanium collector plates on the opposite side of the thruster. They are recessed into the collector side wall and fit snugly. During testing there were two emitters and three collector plates, and the two collector plates nearest to the anode were electrically connected to act as a single collector.

The emitter hollow cathodes are ignited by first supplying a current to the heater coil, which heats the insert to approximately 1000 °C. Next, gas flow is supplied while a potential is applied between the cathode and a collector across the channel. This causes electrons to be thermionically emitted from the insert and then interact with the gas flow, creating plasma inside the cathode tube. At this point the cathode should become self-sustaining and the heater current can be eliminated because plasma ions recombine at the insert, depositing their energy and sustaining the cathode insert temperature required for electron emission. For this experiment, the heater was always energized to keep the cathode emitting. Electrons are pulled through the cathode orifice by the potential between the cathode and collector. Emitted electrons enter the discharge channel, and Hall drift across the channel to the collector.

5. Neutralizer Cathode

The neutralizer was a heated lanthanum hexaboride (LaB_6) hollow cathode flowing xenon. A mass flow rate of 8 sccm-Xe was typical. The heater current was constant at 8 A and the cathode-to-ground potential was generally greater than -10 V. The neutralizer was mounted on the collector side of the thruster approximately 5 cm to the side of the thruster and 10 cm from the exit plane as seen in Figure 3. Two neutralizers were mounted, but only one was used.

B. Facility

The PHT was operated in chamber 3 at the AFRL. The chamber is 3 m in diameter and 10 m long. Pumping is accomplished with a mechanical pump, turbomolecular pump and eight cryopanels. The base pressure is approximately 1e-7 Torr and background pressure during operation was between 8e-6 and 2e-5 Torr. The cryogenic pumps have a total pumping capacity of 150,000 l/s on xenon. The chamber is equipped with a thrust stand, scanning Faraday probe, and retarding potential analyzer (RPA). The faraday probe and RPA are mounted to a motor and rotate 180˚ around the thruster. The chamber walls and cryopanels are shielded with 13 mm thick 99% pure carbon plates to minimize back-sputter.

C. Diagnostics

The plasma diagnostics used to study the PHT were an RPA, Faraday probe, and channel wall probes. Furthermore, the voltage and current of all PHT components were also monitored to assess the operation of the device. The following sections describe the plasma probe diagnostics used in this investigation.

1. Retarding Potential Analyzer

An RPA is utilized to analyze ion voltage distributions downstream of the PHT. In an RPA, a series of biased grids selectively filter ions from reaching a current-measuring probe depending on their energy-to-charge ratios. Specifically, the derivative of the resulting I-V characteristic is proportional to the ion voltage distribution function. Of primary importance for the research presented here is the voltage value for the peak in the distribution function and the width of the distribution at half the maximum value, otherwise known as the most-probable-voltage and full-width half-maximum (FWHM), respectively.

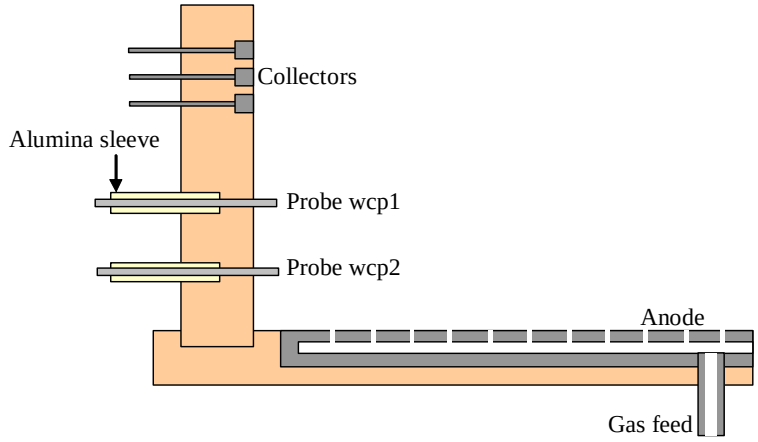

Figure 4. Cutaway view of the PHT showing anode and wall probe detail.

The RPA used for these experiments had three grids: electron repelling; ion retarding; and electron suppression grids. The electron suppression grid was biased at a constant -15 V with respect to ground, while the electron repelling grid was biased to -30 V with respect to ground. RPA data are acquired on centerline of the thruster and ion retarding grid voltage sweeps of 0 to 200 V were used because the discharge voltage was never greater than 150 V.

2. Faraday Probe

A Faraday probe is a type of plasma diagnostic that is often used to measure the ion beam current density profile of Hall thrusters. It consists of a planar metallic electrode that is biased in the ion saturation region. The probe is swept through the thruster plasma plume and current measurements are taken as a function of angular position. This procedure reveals the plume profile of the thruster. For the experiments presented here, the Faraday probe was a 2-cm-diameter electrode spray-coated with tungsten to minimize secondary electron emission. A guard ring surrounding the probe was also used to establish a planar sheath and minimize edge effects. Both the probe and guard ring were biased at -20 V with respect to ground. Previous experiments have shown this to be sufficient for the probe to be in the ion saturation regime. Collected current is measured across a shunt resistor and current density is calculated by dividing by the known probe area.

3. Channel Wall Probes

The channel wall probes are made of 1-mm-diameter tungsten wire. They are positioned 2.5 cm and 5 cm from the anode. Each probe fits snuggly through a hole in the channel and protrudes 2 mm into the discharge volume. A schematic is shown in Figure 4. These probes where used to measure the plasma floating potential at different locations within the discharge channel. In this experiment, no Langmuir probe traces were taken.

D. Setup and Procedure

The PHT was installed on the AFRL thrust stand in chamber three of the PRSS building at Edwards Air Force Base. An aluminum mounting plate was attached to the thruster on its front face. The neutralizer was connected to the stand, but not directly to the PHT. It was mounted on the collector side of the PHT as seen in Figure 3b. The experiment was limited to three mass flow controllers, so both emitters were supplied by the same 50 sccm controller. The anode used a 250 sccm controller, and the neutralizer cathode used a 20 sccm controller. During testing, each data point took approximately five minutes to record; limited by the speed of the rotary motion feedthrough. No value varied more than 5% during the Faraday probe and RPA sweeps. Overall, the thruster ran stably for over ten hours. The Faraday probe was swept in 180° across the centerline of the channel to measure the current density distribution as a function of position, while the RPA was positioned on centerline to record the ion voltage distribution function.

III. Results

Stable operation of the PHT was obtained for a variety of operational configurations. Discharge voltage was varied between 50 - 150 V. Larger voltages were not investigated because the thruster collector electrodes reached thermal limitation. The following sections describe the general operation procedure and the effect of certain key parameters on thruster operation.

A. Start-up and General Operation

The PHT neutralizer and channel emitter cathodes were initially conditioned to prevent poisoning and permanent damage. Each of the two emitters was heated by a variable AC power supply, while the neutralizer cathode was heated with a DC supply. Current was incrementally increased to the maximum value at approximately 0.5 A every

15 minutes. The neutralizer maximum heater current was set at 8 A, while the emitters were each operated with 7.5 A of AC current. Current was continuously supplied to heat all cathodes during all the experiments. It was determined that the neutralizer cathode would not operate without the heater. Operation of the emitters without heater current was not attempted.

After the cathodes were heated, the neutralizer was ignited by supplying propellant and applying voltage to the igniter electrode. The neutralizer would typically ignite when there was 200 V between cathode and igniter. Neutralizer flow rate was always set at 8 sccm-Xe. The cathode-to-igniter current was set at 0.3 A for all experiments. Larger currents were possible, but the igniter is not designed to maintain the cathode discharge, so over-heating the igniter was a concern.

Next, the emitter cathodes were ignited by supplying 25 sccm-Xe (Note: this is total emitter flow rate, we assume it is split 50/50 between the two emitters) and applying a potential between each emitter and its corresponding collector electrode. Emitter two (connected to a higher-power supply) would ignite first, followed by emitter one. In general, decreasing or increasing the flow from this optimum value made it more difficult to ignite the emitters. At this point in the start-up sequence, plasma was visible across the planar thruster channel. The emitters were operated in both a voltage-limited and current-limited mode. During current-limited operation, increasing emitter flow rate would decrease emitter voltage. In voltage-limited mode, increasing emitter flow rate would increase emitter current. This is standard behavior for any hollow-cathode emitter.

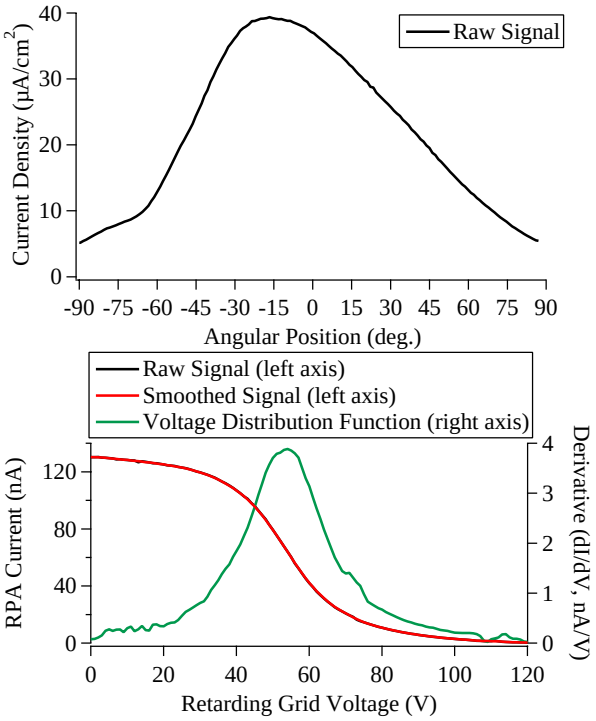

Figure 5 Example traces from the Faraday probe (top) and RPA (bottom) with the ion voltage distribution function.

The next step in the start-up procedure was to apply anode voltage without magnetic field. As anode voltage increased, anode current increased and the visible plasma shifted toward the exit-plane and out of the channel of the thruster. Increasing anode voltage would decrease emitter voltage or increase emitter current, depending on whether the emitters were in current- or voltage-limited mode, respectively. The anode voltage was typically increased to 50 V before proceeding with the next step in the start-up sequence. At this point, anode propellant flow was not present and not necessary for thruster operation.

Finally, the magnetic field of the thruster was added. As magnetic field increased (electromagnet current increased) the discharge current decreased. Also, as magnetic field increased the emitter voltage increased or current decreased, depending on current- or voltage-limited mode, respectively. At this point, all thruster components were energized and active, so data collection and study of the system could begin.

B. Plume Profiles

Faraday probe data sweeps were taken through the plume of the thruster, while the RPA was positioned on centerline to record the ion voltage distribution function. Typical results are shown in Figure 5.

For all investigated operating configurations, the plume profile shows a peak at negative angular positions. Negative angular positions are on the side of the thruster with the collector plates and neutralizer cathode. In the following sections, the angular location at which the peak current density occurs is analyzed as a function of thruster operation. For the RPA data, the peak in the voltage distribution function (i.e., most-probable ion voltage) and the FHWM of the distribution are shown as functions of thruster operation.

Figure 5 shows that the beam current density is asymmetric with respect to the thruster centerline (0 deg). For state-of-the-art annular HETs, the current density distribution typically shows a double peak on centerline, representing each side of the annular channel. Ideally, the PHT would show a flat profile. We have identified several possible explanations for the off-centerline peak in current density: 1) ion creation and acceleration is

occurring primarily at the emitters, 2) space-charge build-up at the collectors, and 3) non-symmetric virtual cathode line formation due to crossed-B electron retardation. The first explanation assumes that a large number of ions are created at the emitters and subsequently accelerated downstream by both the anode voltage and emitter voltage. Therefore, expelled ions are given axial acceleration by the anode and cross-channel acceleration by the emitters. The resultant velocity vector would not be purely axial, resulting in a peak off-centerline.

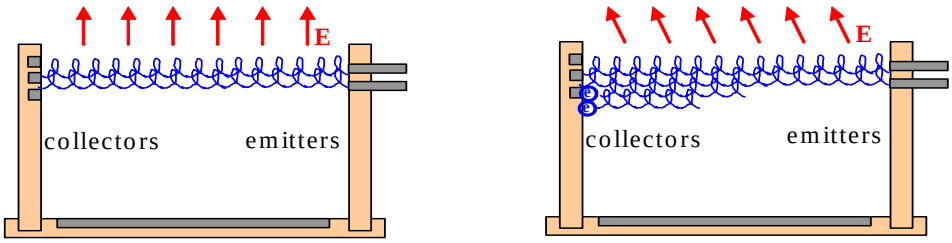

Figure 6. Ideal operation (left) versus non-ideal operation (right).

The second explanation is more plausible. As primary electrons leave the emitters and begin Hall drifting across the channel, they have collisions with neutral atoms expelled from the emitter or anode. The products of these collisions are an ion and secondary electron. The ion quickly accelerates out of the thruster, while the primary and secondary electron remain trapped in the Hall drift. As we proceed across the channel, the number of secondary electrons increases because more collisions have occurred between the primary electron and neutral atoms. Since the emitter-collector circuit is closed, any secondary electrons liberated in the acceleration region (i.e.; not injected through the emitter orifice) cannot be collected by the plates. In other words, the current leaving the emitters is equal to the current being collected by the collector electrodes on the opposite side. Therefore, the excess electrons will be forced to impact the wall and cascade to the anode. The excess electrons on the collector side may cause more ion production on that side of the channel. Further, the potential on the collector side will be lower due to the excess electrons. Therefore, the potential profile across the channel will not be planar and straight, but bowed down near the collectors. This effect will setup an electric field that accelerates ions in both the axial and cross-channel directions. The difference between ideal (no ionization in the acceleration region) and non-ideal (collector wall charging) is depicted in Figure 6.

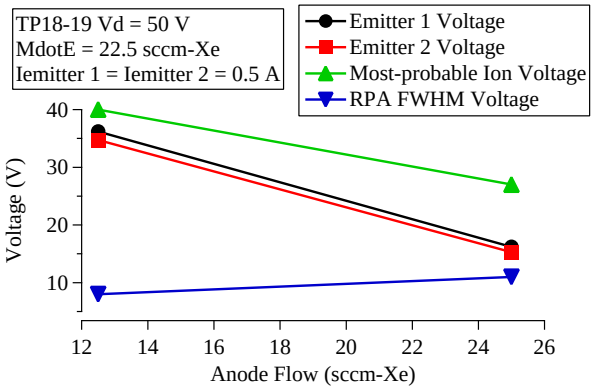

Figure 7. Effects of anode mass flow rate on emitter floating potentials and RPA signal.

Furthermore, electrons generated in the far-field by the neutralizer cathode are inserted into the chamber on one side of the thruster assembly. The local B-field orientation is such that these electrons must collisionally move across field lines to setup the virtual cathode plane where the potential will come to zero. It is conceivable that neutralizer electrons were not able to easily reach the emitter side of the channel; thus, setting up a skewed plane of zero potential at the thruster channel exit. The fact that the ion beam angle is slightly skewed towards the cathode neutralizer location suggests that this effect may also be playing a role. Future investigations will relocate the neutralizer cathode on the opposite side of the thruster or below to examine influence on plume divergence.

C. Parametric Investigation:

The following sections describe specific trends determined from the data acquired during experimental testing. Specifically, trends associated with changes in anode flow rate, emitter flow rate, magnetic field, and emitter current are described. In the plots that follow, the annotation gives the thruster operating point (TP).

1. Anode Flow Rate

The PHT was operated at different anode flow rates. Figure 7 shows the effect of anode flow rate on emitter floating voltage, most-probable ion voltage, and FWHM signal of the RPA. These results are for TP 18 and 19, which had a total emitter flow rate of 22.5 sccm-Xe. As anode flow rate increased, the emitter floating voltages decreased along with the most-probable ion voltage (peak in ion voltage distribution function). The FWHM of the RPA signal increased slightly. Figure 8 shows the effect of anode flow on the wall potentials throughout the

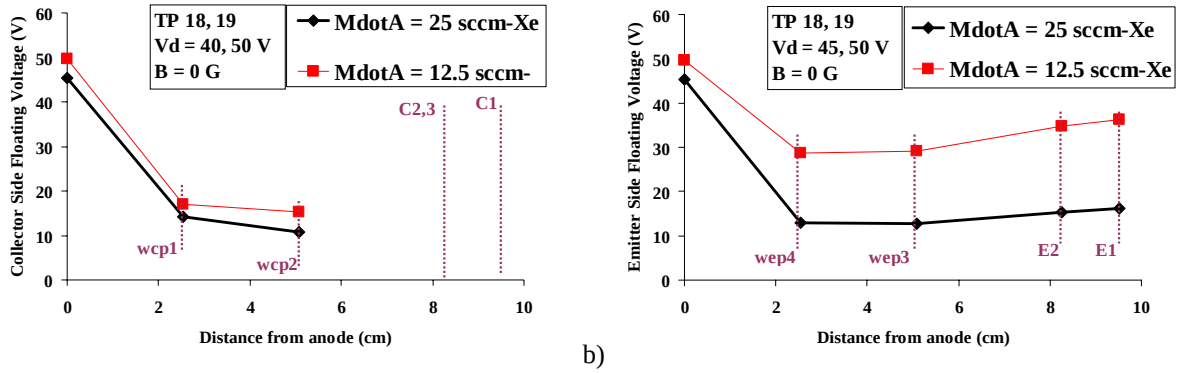

a) b)

Figure 8. Channel floating voltages for a) collector and b) emitter side of the discharge channel for high and low anode mass flow rates without magnetic field.

channel. The x-axis is the axial distance downstream of the anode, and the wall probe and emitter locations are labeled.

As flow rate increases, plasma production is expected to increase and more electrons should be present in the discharge channel. The presence of more electrons will cause the floating potential to decrease and this is shown in both Figure 7 and Figure 8 because increasing anode flow rate decreases floating potential. These trends are expected and controllable with the PHT system. The increase in control with this type of system will allow better understanding of the complex electron transport in HETs.

2. Emitter Flow Rate

An experiment was conducted to determine the effects of emitter flow rate on various discharge and emitter parameters. In an ideal PHT, propellant flow to the channel wall emitters would not be required. Electrons would simply appear at the wall and drift across the channel. Total emitter flow rate was normally held constant at 22.5 sccm-Xe. In this experiment, the emitter flow rate was reduced, while monitoring the discharge and emitter properties. Note that the total emitter flow rate is assumed to be split 50/50 between each of the two emitters. Figure 9 shows the results.

In Figure 9a, the emitter floating potential and potential difference between emitter 1 and 2 are shown as a function of emitter flow rate. As flow rate decreases, the floating potential of the emitters increases. This is expected since less propellant flow causes the plasma electron density to decrease, which results in a higher floating voltage. The potential difference between the two floating emitters remains relatively constant during this procedure. These data are for a discharge voltage of 150 V, 20 sccm-Xe anode flow, emitter 1 at 1.3 A, and emitter 2 at 1 A. Also, the most-probable ion voltage from the RPA data shows that ions have a voltage almost identical to the emitter 1 floating potential. This suggests that most of the ions are being created at the emitter 1 axial location, in the acceleration region of the PHT.

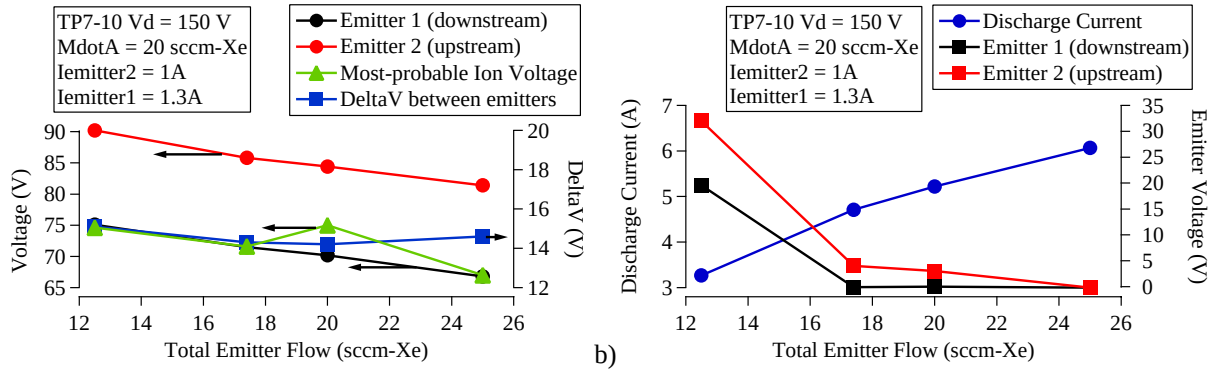

a) b)

Figure 9. Effect of emitter flow on a) emitter floating potentials and b) discharge current and emitter operation voltage.

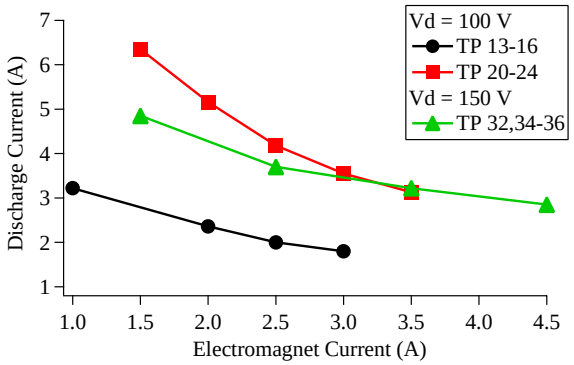

Figure 10. Discharge current as a function of electromagnet current for various operating conditions.

Figure 9b shows the change in discharge current and emitter operating voltage as emitter flow changes. When emitter flow decreases, discharge current decreases and the emitter operating voltage increases. Because the emitters are operating in a current-limited mode for this experiment, as the flow rate decreases more voltage is required to maintain the current. Further, as flow rate decreases the discharge current decreases because less plasma is created due to less neutral gas.

3. Magnetic Field

The PHT was also operated with different magnetic flux densities to analyze the magnetic field effects on thruster operation. In traditional annular thrusters, the magnetic field is set to minimize the discharge current. Typically this yields the best thruster performance. This procedure was attempted but not realized for the PHT. Specifically, as the magnetic field was increased, the discharge current did decrease. However, it never reached a minimum. Instead, it continued to decrease with increasing magnetic field. This trend is shown in Figure 10.

Figure 11 shows voltages as a function of distance and magnetic field strength along both thruster side-walls (refer to Figure 8for probe and emitter locations). Figure 11a shows changes in potential on the collector side of the thruster. The anode is at 100 V and the floating probes record values between 40-60 V. On the emitter side of the thruster channel, (Figure 11b) a decrease in potential between the emitter and anode location is observed. As magnetic field increases, the floating probe potential decreases slightly. At the collectors, the floating potential drops substantially as magnetic field increases. This is caused by better confinement of electrons as magnetic field increases. This also causes the floating potential of the wall probes to decrease as magnetic field increases.

Figure 11b shows changes in potential on the emitter side of the thruster. A steep potential well is observed between the anode and emitters. As magnetic field increases, floating potential of the wall probes increases because more electrons are confined to traverse across the channel and have a more difficult time getting to the emitter-side wall.

The application of the magnetic field across the channel caused retardation of electrons and a stable acceleration region. Ion energies between 50-65 eV were obtained with a peak in flux distribution 15-20º "off-axis" for 100 V discharge operation. Figure 12 shows RPA and Faraday probe data for several test points including emitter floating voltages in the acceleration channel. Plume variation across the minor axis of the thruster was not tested.

As magnetic field increased, the emitter floating voltage decreased. This is consistent with previous results. As magnetic field increases, electron motion across the channel is impeded, which results in a build-up of electron density. The higher electron density results in a lower floating potential. The most-probable ion voltage is always

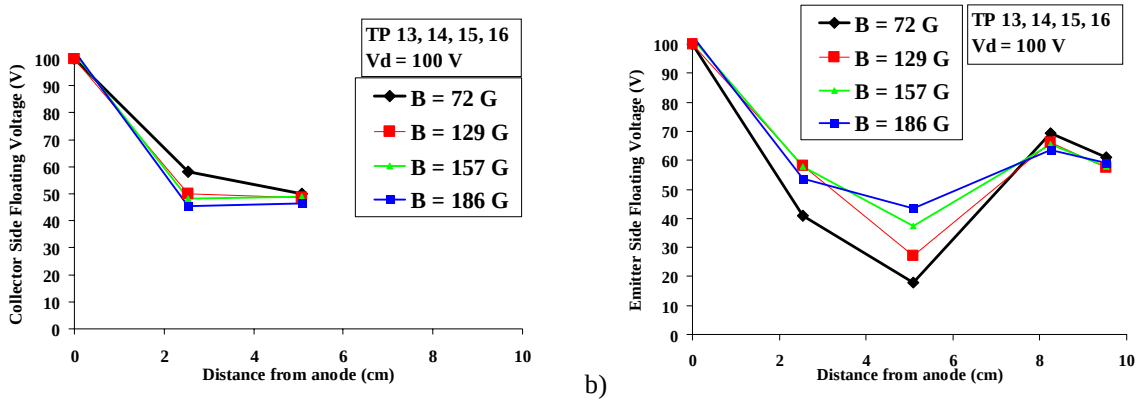

a) b)

Figure 11. Floating voltages for V_d = 100 (V) and various magnetic fields for the a) collector and b) emitter side of the thruster channel.

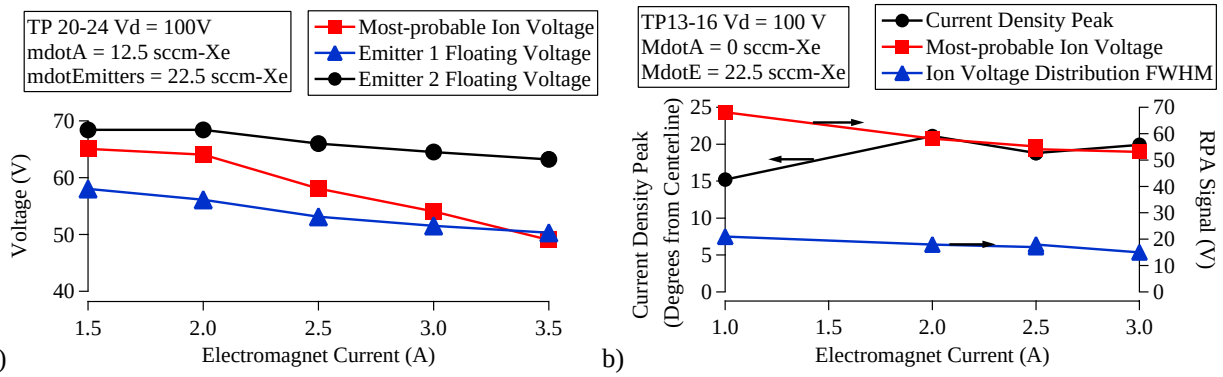

Figure 12. RPA and Faraday probe measurements for V_d=100 (V) and various magnetic field strengths with and without anode flow.

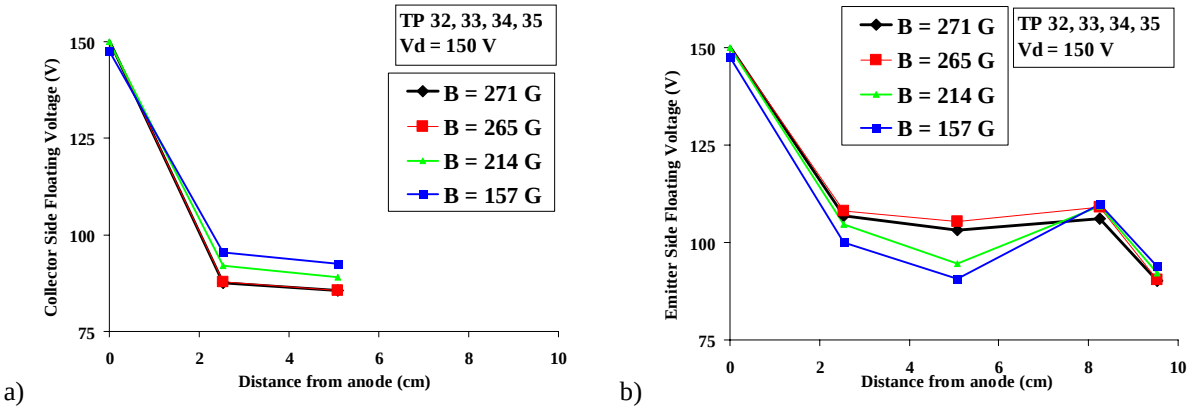

Figure 13. Floating voltages for V_d = 150 (V) and various magnetic field strengths for the a) collector and b) emitter side of the channel.

between the emitter 2 (upstream) and emitter 1 (downstream) floating potentials. This result suggests that ions are being created in the acceleration region and are, therefore, not gaining the full acceleration of the discharge voltage. This result is expected since the mass flow rate through the emitters was larger than the anode. Experiments attempting to reduce emitter flow rate and increase anode flow rate were attempted. However, the emitters require a minimum mass flow rate to operate and a complete investigation was not possible due to mass flow controller limitations. Future experiments are being planned to study this effect. Operation at a higher anode voltage of 150 V produced similar results to the 100 V operation point.

Figure 13 shows the floating voltage profile across the channel length showing an acceleration region voltage peak of about 100V. RPA and Faraday probe data similarly shows most probable ion energies of 85-95 eV and an off-axis peak in current distribution at 10-15°.

4. Emitter Current

Before the end of the short testing period, there was a brief look into the effect of changing the emitter currents relative to one another. At a thruster setting of 100 V, 5 A, and B_{max} of 100 gauss, the ratio of emitter 1 driving voltage to emitter 2 driving voltage was varied. Figure 14 shows the data obtained. It is interesting that the most probable ion voltage is bounded by the two floating voltages. This indicates that the thruster is not operating ideally because ions are born somewhere in the acceleration region. The figure also shows two interesting facts of PHT operation. Firstly, the emitter (and in turn Hall) currents can be adjusted independently. This should allow the operator to dial in an array of axial electron density profiles. Secondly, it shows that the ion voltage has a stronger dependence on emitter conditions when they are operated similarly. This is important because it shows that attempting to induce a sharp axial change in n_e is not beneficial. The idea hints that multiple emitters are likely favored.

This type of emitter current experiment must be carried out in more detail, preferably with more collector-emitter pairs. As shown in Figure 14, the most probable ion voltage varied while the thruster conditions (discharge voltage,

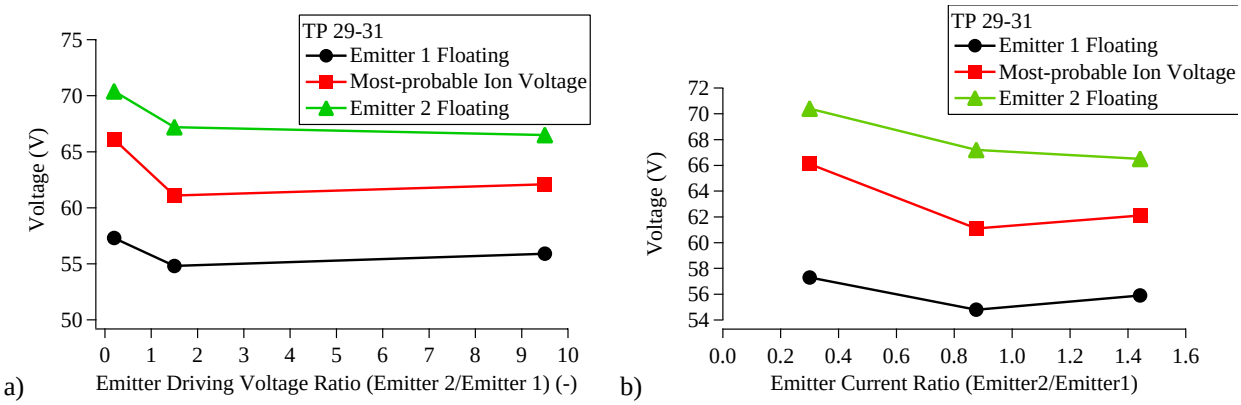

Figure 14. Effect of changing relative emitter settings on floating voltage and ion voltage.

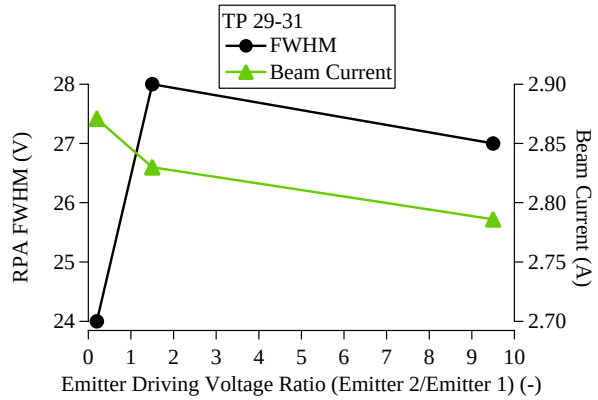

Figure 15. Effects of changing emitter driving voltage on ion voltage distribution function FWHM and Faraday probe integrated beam current.

discharge current and magnetic field) were held constant. Further investigation is needed to determine if this change in ion energy is due to electric field structure, electron mobility, increased ionizations, or a combination of these.

Also of note is the effect of relative emitter characteristics on the plume. The RPA data show that as the emitter driving voltage ratio (emitter 2/emitter 1) increased, so did the FWHM of the RPA scan. The RPA output is shown in Figure 15. In addition, the difference in emitter floating voltages decreases. With a smaller range of voltages between the emitters (where most of the ionization is believed to occur) the RPA collected a boarder range of ion voltages. These data imply that higher thruster performance requires the strongest region of the electric field to be at the most downstream location.

IV. Conclusions

Stable operation of a Hall thruster that emits and collects the Hall current in a plane across a linear discharge channel has been demonstrated. The PHT is being investigated for use as a test bed to study electron mobility in ExB devices. The planar geometry attempts to de-couple the complex electron motion found in annular thrusters by using simplified geometry. During this initial test, the PHT was operated at discharge voltages between 50-150 V to verify operability and stability of the device. Hall current was emitted by hollow cathode electron sources and collected by electrodes on the opposing wall of the thruster. Internal channel wall probes along with a downstream Faraday probe and retarding potential analyzer measured changes in thruster plasma as the Hall current, discharge voltage, magnetic field, and mass flow rates were changed. Results show that most of the plume ions are created in the acceleration zone. Further, increasing the magnetic field confines electrons to the Hall-drift region. This causes the discharge current to decrease, but no minimum in discharge current, which traditionally corresponds to an optimum point, was observed. Future experiments with this thruster are being planned to shed light on electron mobility in both planar and annular ExB thruster geometries.

Acknowledgments

We would like to thank the entire research team at Starfire Industries LLC who have been instrumental in this investigation. Also, the testing would not have been possible without the aid of engineers at AFRL including Dan Brown, Dr. James Haas, and Dr. Brian Beal. This work was supported by DoD SBIR Phase I contract number FA9300-05-M-3009.

References

[1]Ahedo, E., Gallardo, J. M., Martinez-Sanchez, M., "Effects of the radial plasma-wall interaction on the Hall thruster discharge," *Physics of Plasmas*, Vol. 10, No. 8, pp. 3397-3409, 2003.

[2]Meezan, N. B., Hargus, W. A., Cappelli, M. A., "Anomalous electron mobility in a coaxial Hall discharge plasma," *Physical Review E*, Vol. 63, No. 2, Feb. 2001.

[3]Janes, G. S., Lowder, R. S., "Anomalous Electron Diffusion and Ion Acceleration in a Low-Density Plasma," *Physics of Fluids*, Vol. 9, No. 6, pp. 1115-1123, June 1966.

[4]Knoll, A., Thomas, C., Gascon, N., Cappelli, M., "Experimental Investigation of High-Frequency Oscillations within Hall Thrusters," AIAA-2006-5171, *42nd Joint Propulsion Conference*, Sacramento, CA, July 9-12, 2006.

[5]Keidar, M., Beilis, I. I., "Electron Transport Phenomena in Plasma Devices with ExB Drift," *IEEE Transactions on Plasma Science*, Vol. 34, No. 3, pp. 804-814, June 2006.

[6]Raitses, Y., Staack, D., Keidar, M., Fisch, N. J., "Electron-wall interaction in Hall thrusters," *Physics of Plasmas*, Vol. 12, No. 5, May 2005.

[7]Raitses, Y., Smirnov, A., Staack, D., Fisch, N. J., "Measurements of secondary electron emission effects in the Hall thruster discharge," *Physics of Plasmas*, Vol. 13, No. 1, Jan. 2006.